

THESIS FOR THE DEGREE OF LICENTIATE OF ENGINEERING

**A Cross-Correlator for the Remote
Sensing of Earth by Synthetic Aperture**

ERIK RYMAN

Division of Computer Engineering
Department of Computer Science and Engineering
CHALMERS UNIVERSITY OF TECHNOLOGY
Göteborg, Sweden 2011

A Cross-Correlator for the Remote Sensing of Earth by Synthetic Aperture

Erik Ryman

Copyright © Erik Ryman, 2011.

Technical report 12L

ISSN 1652-876X

Department of Computer Science and Engineering

VLSI Research Group

Division of Computer Engineering

Chalmers University of Technology

SE-412 96 GÖTEBORG, Sweden

Phone: +46 (0)31-772 10 00

Author e-mail: eriryman@chalmers.se

Cover:

Picture of the fabricated cross correlator

Printed by Chalmers Reproservice

Göteborg, Sweden 2011

A Cross-Correlator for the Remote Sensing of Earth by Synthetic Aperture

Erik Ryman

Division of Computer Engineering, Chalmers University of Technology

ABSTRACT

In light of our changing climate and the unpredictability of severe weather; a better understanding of our climate and increased weather forecast accuracy are in high demand. Humidity and temperature distribution profiles with high temporal resolution can significantly increase our knowledge of highly dynamic weather phenomena and improve weather forecasts.

Microwave sounding from low earth orbit is extensively used for humidity and temperature measurements in the atmosphere because of its much better cloud penetrating properties compared to visible and infrared light. Performing these observations from geostationary earth orbit (GEO) would give the additional advantage of large coverage and no revisiting times. Microwave sounding from GEO is however demanding, this because of the large aperture required to reach acceptable spatial resolution. Synthetic aperture interferometry, widely used in ground based radio astronomy, has been proposed as a solution to overcome this obstacle.

Cross-correlation is a signal processing algorithm that is a central and highly calculation-intensive part of aperture synthesis. CMOS process technology scaling, and the decreasing power per performance figures that have followed, has finally reached a point where these kinds of instruments are viable for space deployment.

This thesis presents a cross-correlator chip that has been designed, fabricated and extensively evaluated, paving the way for larger correlator systems based on similar design concepts. Routing and synchronization schemes were developed for the purpose of handling the massively parallel calculations and the signal distribution and timing issues specific to synthetic aperture cross-correlators. The chip presented shows significant improvements over previous correlators in power per performance evaluations.

Keywords: Cross-correlation, synthetic aperture, earth observation, ASIC, VLSI.

Preface

Parts of the contributions presented in this thesis have previously been accepted to conferences or submitted to journals.

- ▷ **Erik Ryman**, Anders Emrich, Johan Embretsén, Johan Riesbeck, Stefan Back Andersson, Per Larsson-Edefors and Lars Svensson, “Digital Cross-Correlators: Two Approaches,” in *GigaHertz Symposium*, Lund, Sweden, March 9-10, 2010
- ▷ **Erik Ryman**, Per Larsson-Edefors, Lars Svensson, Anders Emrich and Stefan Back Andersson, “A Single-chip 64 Input Low Power High Speed Cross-Correlator for Space Application,” in *Microwave Technologies and Techniques Workshop*, Noordwijk, The Netherlands, May 10-12, 2010
- ▷ **Erik Ryman**, Anders Emrich, Stefan Back Andersson, Johan Riesbeck, Lars Svensson and Per Larsson-Edefors, “3.6-GHz 0.2-mW/ch/GHz 65-nm Cross-Correlator for Synthetic Aperture Radiometry,” in *IEEE Custom Integrated Circuits Conference*, San Jose, California, USA, September 18-21, 2011

Acknowledgments

I am grateful to the following people for what they have done for me, for my career, and for this thesis.

- ▷ Professor Per Larsson-Edefors for always being available and supporting me with both the technical and academical aspects of my PhD project.
- ▷ Dr. Anders Emrich for all his help and especially for providing deep insight and technical knowledge about the application of my work.
- ▷ Stefan Back Andersson and docent Lars Svensson for sharing their knowledge on circuit design with me.
- ▷ Johan Riesbeck for his help with the ASIC evaluation and setting up a measurement environment.
- ▷ David Runesson for his help with the test board design, Ulrika Krus for her help with the high frequency aspects of designing the test board and Mattias Ericsson for his support with the PCB tools.
- ▷ Magnus Hjorth for his help getting me started in the early stages of correlator design.
- ▷ All the other colleagues at Omnisys Instruments for all the good times at the office and elsewhere.
- ▷ Kasyab P. Suramaniyan for all the good times during the time we shared office, Alen Bardizbanyan and Bhavishya Goel for arranging gokart and paintball activities and all other PhD students at the Division of Computer Engineering for being my friends.

- ▷ Dr. Magnus Sjalander for his friendliness and help with everything FlexSoC related.
- ▷ Lars Kollberg, for his help setting up the ASIC design tools.
- ▷ Rune Ljungbjörn and Peter Helander for their IT support.
- ▷ All colleagues at the Department of Computer Science and Engineering who have helped me with administrative tasks.
- ▷ The Swedish Research Council (VR) for the partial funding of my work under Contract 621-2007-4727.
- ▷ All my friends who have made me endure this far.
- ▷ My parents Eva and Christer Ryman and sisters Anna Ryman and Sofia Augustsson for all their support through my life.

Erik Ryman
Göteborg, November 2011

Contents

Abstract	i
Preface	iii
Acknowledgments	v
I INTRODUCTION	1
1 Introduction	3
1.1 Context and motivation	3
1.2 Correlator system considerations	7
1.3 Problem statement	9
1.4 Custom comparator	10
1.5 Future work	12
Bibliography	13
II PAPERS	15
2 PAPER I	19
Bibliography	21
3 PAPER II	25
3.1 Introduction	25

3.2	Cross-Correlation	26
3.3	The Cross-Correlator Implementation	27
3.4	Performance	29
3.5	Power	30
3.6	Conclusion	32
	Bibliography	32
4	PAPER III	37
4.1	Introduction	37
4.2	Architecture	39
4.3	Implementation	40
4.4	Test Setup	42
4.5	Test Results	43
4.6	Discussion	46
4.7	Acknowledgment	47
	Bibliography	48

List of Figures

1.1	Proposed antenna array of the Geostationary Atmospheric Sounder.	6
1.2	Comparator schematic and connection to cross-correlator.	10
2.1	The FPGA based correlator.	20
2.2	The ASIC correlator.	21
3.1	Schematic of digital cross-correlation.	27
3.2	8-input example of the signal routing.	29
3.3	The cross-correlator layout.	30
3.4	Skew simulation results.	31
4.1	8-input routing example.	41
4.2	2-input correlator schematic.	41
4.3	Test PCB block diagram.	43
4.4	Cross-correlator ASIC mounted on thin-film substrate.	44
4.5	Shmoo plot for performance vs supply voltage.	45
4.6	Clock skew sweep.	46
4.7	Supply current vs frequency and supply voltage.	47

Part I

INTRODUCTION

1

Introduction

1.1 Context and motivation

There is a great need of a better understanding of our changing climate and of improvements in weather forecasting. Increased coverage, accuracy and temporal resolution of atmospheric temperature and humidity measurements could prove a significant aid in developing better weather models. Both National Aeronautics and Space Administration (NASA) and the European Space Agency (ESA) are involved in development of a new generation of weather satellites. These satellites will perform microwave sounding from a geostationary earth orbit (GEO) providing previously unattainable data. Observation in the infrared or visible light spectrum makes it possible to see clouds but what happens inside of these is obscured by the absorption and scattering of light

at these wavelengths. The microwave frequency range, because of the much better cloud penetrating properties, is ideal for satellite measurement of these atmospheric properties.

There are a number of advantages of observation from GEO over low earth orbit (LEO), perhaps most importantly it eliminates the problem of revisiting times, i.e. the time between two consecutive observations of the same spot. When performing observations with satellites in LEO; the satellite will orbit the earth in a predetermined pattern, this makes continuous observation of an area an impossibility. Even worse, when the object of interest is in itself moving, like storms and hurricanes, it becomes a hit or miss game where in the first pass the object might not yet have reached the satellite path and in the next it may already have moved past it. The continuous coverage possible from GEO means the instrument will be the limiting factor for image update frequency, increasing the temporal resolution of observation way beyond what can be achieved from LEO. Another advantage of GEO is that it, due to the very high altitude, enables simultaneous observation of almost the entire hemisphere.

Traditionally, in radio remote sensing performed from satellites, a parabolic dish antenna scanning the surface of the earth, as the satellite passes over it, has been used. The spatial resolution that can be achieved by an antenna of this type is determined by its half power beam width (HPBW). The HPBW of a parabolic dish antenna can be approximately described by $HPBW(\text{degrees}) \approx 70\lambda/D$ where λ is the wavelength of the observed radiation and D is the aperture of the antenna [1]. Observation at lower frequencies means larger apertures are required to retain the same HPBW.

The considerably higher altitude of GEO (35,786 km), compared to polar orbits (commonly around 1,000 km), demands a much more narrow beam width if the spatial resolution is to be retained. The requirement of a narrow beam width combined with microwave frequencies down to the 50 GHz range amplifies the aperture requirement. A real aperture antenna would have to be larger than 8 m to give a spatial resolution of 35 km at 50 GHz from GEO. Such large aperture antennas are impractical for space application, because of both their weight and their size.

Interferometric aperture synthesis has been used by radio astronomy observatories for decades and is increasingly used as a means to surpass the performance of real aperture telescopes. The Very Large Array (VLA) in New Mexico has been using synthetic aperture since 1980 [2]. It consists of 27 telescopes placed in a Y-shape where each arm can be extended to 21 km giving a resolution similar to a 36 km real aperture antenna. The Atacama Large Millimeter/submillimeter Array (ALMA) is currently under construction in the Atacama dessert in Chile [3]. In September 2011 it opened for observation on a reduced number of telescopes and acquired its first pictures [4]. When fully operational the ALMA observatory will have 66 antennas. The Square Kilometer Array (SKA) is in the planning stages, if constructed, it will have a combined collecting area of one square kilometer making it the most sensitive interferometer by a great margin [5].

The usage of interferometric sounding for remote sensing of the earth was conceived of as early as 1988 [6]. By placing the numerous smaller receiver elements placed on arms that can be folded during launch both the weight and the size of the instrument can be significantly reduced compared to a real aperture alternative, enabling such an instrument to be launched into space.

The Soil Moisture and Ocean Salinity (SMOS) satellite carried the first polar orbiting correlator for synthetic aperture. It was launched by ESA to LEO in 2009 [7]. With its orbital height of 770 km it is considerably closer to the surface than GEO and thus requires less receiver elements [8]. It has a Y-shaped array, similar to that of the VLA, consisting of 69 receiver elements placed on three foldable arms for easier deployment.

An additional advantage of using synthetic aperture, aside from weight and easier deployment, is that it provides an image of the observed area where all parts are simultaneously acquired. In contrast, a scanning approach will introduce time skew between the first and last part of a picture.

There are currently two projects aiming at producing GEO microwave sounding instruments. The Geostationary Atmospheric Sounder (GAS) is being developed by Ruag Space AB and Omnisys Instruments AB. It will perform synthetic aperture radiometry using a Y-shaped rotating array of receiver elements,

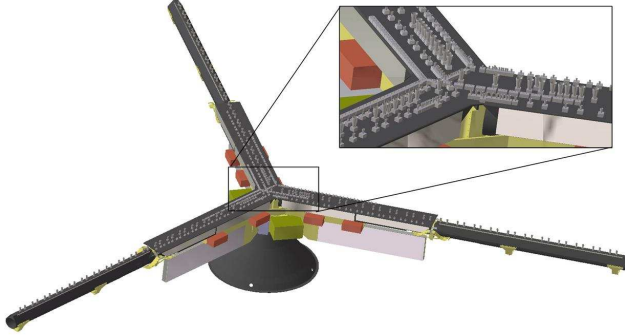


Figure 1.1: *Proposed antenna array of the Geostationary Atmospheric Sounder.*

Fig. 1.1. It will operate in the 53, 118, 183 and 380 GHz bands to give vertical temperature and humidity profiles under all weather conditions. A demonstrator of the GAS concept with 21 receiver elements in the 53 GHz band has been constructed [9]. Outdoor tests of this demonstrator were carried out with very promising results during 2010. Preliminary specifications of the final instruments suggest it would need in the order of 136 receiver elements in the 53 GHz band alone [10]. On top of this the instrument will also have around 107 receivers for each of the 118, 183 and 380 GHz bands. To further increase the accuracy the receiver array will be rotating, sampling even more baselines.

The Geostationary Synthetic Thinned Aperture Radiometer (GeoSTAR) is a NASA led instrument project similar to GAS. It will operate in the 50 GHz range for temperature measurements and 183 GHz range for water vapor measurements. GeoSTAR will have a non-rotating Y-shaped array with significantly more receiver elements than GAS, preliminary figures suggest up to 300 for the 50 GHz band [11]. A GeoSTAR prototype has been constructed and produced its first images in 2005 with excellent results [12].

1.2 Correlator system considerations

The GAS and GeoSTAR prototypes have paved the way for future full sized instruments, demonstrating the maturity of the technologies involved. There are still, however, remaining challenges to overcome. Calculation intensity when reconstructing the observed image is one of the limiting factors to the usage of aperture synthesis in space. Sending the raw data to ground, performing the calculations there, is not feasible, as the raw data bandwidth required would be in the order of hundreds of gigabits per second. The discrete cross-correlation algorithm, Eq. 1.1, is one important step of reconstructing the observed image from an aperture synthesis instrument. Two signals f and g are multiplied at different time lags m and integrated over time (or samples) n . The integrating part of the algorithm will have a mitigating effect on the amount of data. Depending on integration time N it can reduce the bandwidth by order of magnitudes. Cross-correlation is performed pair-wise on all, or a subset of the signals from the receivers.

$$(f * g)[m] = \frac{1}{N} \sum_{n=0}^{N-1} f[n]g[n + m] \quad (1.1)$$

The problem of performing the calculations in space is mainly one of power dissipation. While ground based radio observatories can rely on powerful computers to perform the task of signal processing a satellite has a much too limited power budget for the same kind of approach. Even moderately power hungry approaches suffer from the problem of cooling in a vacuum environment. Heat generated within a satellite has to be transported to the outer casing and radiated away. If heat starts to build up in critical areas it can have detrimental effects, instrument sensitivity can be lost due to noise, temperature drift can cause unstable measurement results and severe thermal gradients may even cause structural failure.

There are two common types of cross-correlator systems, XF and FX, which basically differ in the order they perform the signal processing. Whereas the FX correlator first performs a Fourier transform and then a cross-correlation, the XF does the other way around. While both types perform the same job, the impact

the different approaches have on the system design differs greatly. The correlator presented in this work is of the XF variety. This makes it possible to perform the cross-correlation on the satellite and all other signal processing on ground. The cross-correlation algorithm in an XF system samples the complex valued visibility function which is the spatial Fourier transform of the real valued intensity image. The intensity image can then be obtained from the cross-correlated data through post-processing.

The maximum clock frequency of the digital cross-correlator determines its bandwidth. In a real valued cross-correlator the bandwidth available is half of the clock frequency. For a complex-valued correlator where the input signals are split into I and Q components, double the bandwidth of the real valued correlator can be achieved while sacrificing half of the correlator inputs. If further bandwidth requirements are needed, time demultiplexing techniques can be used, increasing the number of signals to be correlated even further.

A digital cross-correlator will have to operate on quantized signals and, thus, the number of quantization levels will affect the signal to noise ratio. A sampling accuracy of only one bit (two-level quantization), where no amplitude information is captured, can in many cases be sufficient. Compared to a full precision sampling (infinite-level) correlation the signal to noise ratio is 64 % [13]. For a three-level correlator it increases to 81 % and at four levels it reaches 88 %. While the signal to noise improvement is not dramatic the correlator power consumption and area could almost double for a four-level system compared to a two-level system.

The number of lags in each cross-correlation determines the frequency resolution available in the acquired image. A zero-lag correlator gives a brightness temperature at only a single frequency. In many cases this can be enough. The chip area will increase almost linearly with the number of lags applied, since multiplication and integration will have to be performed for every extra lag introduced.

The resolution and unambiguous field of view (FOV) is determined by the number and distribution of receiver elements. A large FOV (17° for whole hemisphere seen from GEO) requires small antenna spacings or baselines. The

resolution is determined by the long baselines. When combining a large FOV with a high spatial resolution the number of elements, and thereby the number of input signals, required will be large, putting extra demand on the cross-correlator system.

Longer integration times reduces noise while also reducing image update frequency. The integration time possible is determined by the number of integration bits in combination with correlator clock frequency.

1.3 Problem statement

The cross-correlator presented in this work was to be a proof-of-concept and as such it had to be sufficiently large to test the design ideas developed but still small enough to be economically viable. The total number of correlation products, or channels, can be expressed by $ch = n(n - 1)/2$ where n is the number of inputs. As seen the number of channels grows quadratically with the number of inputs. We settled for a design with 64 inputs (which can also be used as a 32-input correlator in complex mode), this translated to 2016 unique signal pairs to be cross-correlated. It was also decided to go for 1-bit accuracy, 0-lag correlation and 30 bit integration. As well as meeting the above mentioned requirements this also meant the cross-correlator was made to the same specifications as a previous, FPGA-based, correlator developed at Omnisys, this was useful for comparison reasons. For the chip to demonstrate the viability of the interferometric synthetic aperture approach it had to show significant improvements in power per performance figures compared to previous correlator systems, while also demonstrating a design that could be scaled to accommodate the larger number of signals in future ventures.

An application specific integrated circuit (ASIC) cross-correlator has been fabricated and extensively tested. The design ideas, challenges and test results are presented more in depth in the papers included in this thesis. A custom comparator, presented in the next section, has been designed for the purpose of performing the AD conversion and sampling required in a cross-correlator system.

1.4 Custom comparator

In testing the correlator ASIC commercial off-the-shelf comparators were used [14]. When constructing the test platform a number of limitations were found that eventually led to the decision to design a custom comparator for the next generation cross-correlator system. One of the main concerns was power consumption, the comparators used on the test board were single channel and each used 140 mW of power. In a system requiring hundreds of comparators this would not work, but the power consumption has to be drastically reduced. Another consideration was the system level integration. A system using hundreds of single channel comparators will become very large and complex. Multi channel comparators will have a smaller total footprint, which will reduce both size and weight of the system. The reduced footprint will also make it possible to place the comparators closer to the cross-correlator ASIC, this means additional power can be saved by scaling down driver strength. With shorter interconnect lengths between comparator and correlator, noise and losses will be reduced. Overheads such as clock distribution and biasing will also go down, saving even more on power consumption. Finally making a custom ASIC would make it possible to add features such as input offset adjustment, power tuning and adapting the input and output levels to fit within the correlator system.

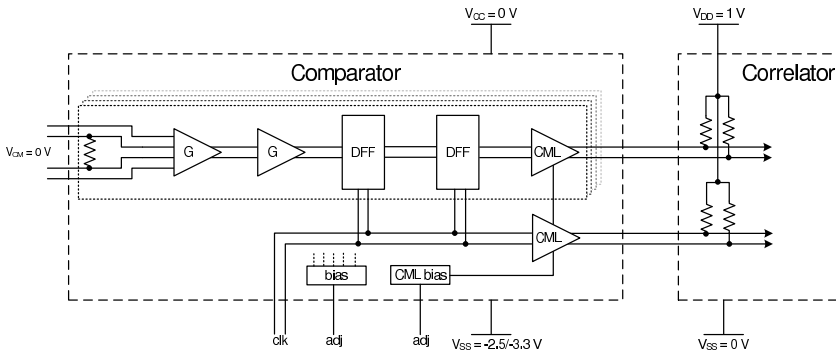


Figure 1.2: Comparator schematic and connection to cross-correlator.

The Comparator was constructed in a high speed 130 nm SiGe Bi-CMOS process from STMicroelectronics. The entire comparator is using differential signalling and all transistors are bipolar. An 8-channel design was decided upon as a compromise between the previously mentioned system complexity issues and the costly chip area. This decision also fitted well with the current cross-correlator ASIC which uses one clock for every 8 data channels. A $100\ \Omega$ resistor between the input ports is used for LVDS compatible termination. The comparator is constructed to operate on negative supply voltages between $-3.3\ \text{V}$ and $-2.5\ \text{V}$. Having the considerably lower supply voltage correlator at positive supply and the comparator at negative supply makes it possible to connect the two together without any level translation circuitry. A CML driver on the output of the comparator is simply terminated to the correlator supply voltage instead of ground, giving an output voltage swing lying within the correlator ASIC supply range. To move the upper limit of the common mode range of the inputs above $0\ \text{V}$ emitter followers were inserted as a first step, this moving of the common mode range makes it possible to use ground as a reference level for the system. Two Gilbert gain amplifiers, because of their flat frequency response, were connected in series to amplify the signal to levels required for the sampling circuit. The first amplifier has an extra pair of inputs for offset adjustment, these are connected to a transistor pair parallel to the ones of the signal inputs. Having some way of adjusting offsets is an important part of tuning the correlator system. The comparator used in the cross-correlator test setup had a single latch which meant the cross-correlator had only half a clock cycle to correctly detect the incoming data. The sampling in the custom comparator is performed by two latches in series, with opposite clock phases, forming a flip-flop.

Two current mirror biasing circuits are used for all channels in common, one for setting CML output driver current and one for all remaining logic. Both biasing circuits have an external control pin making it possible to tune the comparator for different performance, drive strength and power dissipation needs. Both pins can be left unconnected if no tuning is needed. A clock return output was also included so that a clock signal can be routed together with data, to be connected to the cross-correlator chip.

Isolation between the different input signals is an important aspect. To Achieve a good isolation one V_{SS}/V_{CC} pin was inserted between each input channel. A dense power supply mesh forms an additional wall between all channels inside the ASIC. Common centroid design practices were applied to decrease offset drift caused by temperature gradients.

Simulations suggest the comparator will correctly sample a 1 mV_{p-p} , 2.5 GHz differential input signal, this with a clock speed of 5 GHz, a supply voltage of 3.3 V and default biasing. The supply current in this case is 9 mA/channel making for a power consumption of 30 mW/channel. The output swing would be around 350 mV with $50\ \Omega$ terminated to 1 V. The common mode range of the comparator, according to simulation, is -1.3 V to 0.5 V at -3.3 V supply.

1.5 Future work

While the cross-correlator ASIC demonstrates the validity of the design ideas introduced in this work, it is still a large way away from a full scaled correlator system. An increased number of inputs to the ASIC is required for accommodating future ventures. Dividing the workload between multiple ASICs, one might suggest even the current correlator would suffice. However, in a system where all correlation products are to be calculated, halving the number of inputs leads to at least a fourfold increase in the number of chips required. For example a relatively small correlator system with 128 receivers would require more than 16 of the current ASICs to accommodate all correlation products. The increased number of ASICs leads to a correspondingly increasing number of interconnects between chips. Inter-chip interconnects require much more power than intra chip interconnects; the total power required will rise. From a system perspective the increased power requirements and signal routing complexity that will follow could kill the entire application. A future larger cross-correlator ASIC will have to balance the cost of producing larger dies with system level considerations.

The correlator ASIC in itself does not constitute a complete correlator system. There are many other considerations for a complete correlator system

such as signal integrity, sampling, PCB routing, packaging, control and external communication. The 8-channel comparator, performing the task of digitizing the signals in a future correlator system, will be tested and presented in future work.

Bibliography

- [1] R.E. Collin, *Foundations for microwave engineering*, IEEE Press series on electromagnetic wave theory. IEEE Press, 2001.
- [2] P.J. Napier, A.R. Thompson, and R.D. Ekers, “The very large array: Design and performance of a modern synthesis radio telescope,” *Proceedings of the IEEE*, vol. 71, no. 11, pp. 1295 – 1320, November 1983.
- [3] A. Wooten and A.R. Thompson, “The Atacama Large Millimeter/Submillimeter Array,” *Proceedings of the IEEE*, vol. 97, no. 8, pp. 1463 – 1471, August 2009.
- [4] “ALMA Opens Its Eyes,” <http://www.almaobservatory.org/en/press-room/press-releases/297-alma-opens-its-eyes>, October 2011.
- [5] R. Mittra, “Square Kilometer Array-A unique instrument for exploring the mysteries of the universe using the Square Kilometer Array,” in *Applied Electromagnetics Conference (AEMC)*, December 2009, pp. 1 – 6.
- [6] C.S. Ruf, C.T. Swift, A.B. Tanner, and D.M. Le Vine, “Interferometric synthetic aperture microwave radiometry for the remote sensing of the Earth,” *IEEE Trans. on Geoscience and Remote Sensing*, vol. 26, no. 5, pp. 597 – 611, September 1988.
- [7] J. Font, A. Camps, A. Borges, M. Martín-Neira, J. Boutin, N. Reul, Y.H. Kerr, A. Hahne, and S. Mecklenburg, “SMOS: The Challenging Sea Surface Salinity Measurement From Space,” *Proceedings of the IEEE*, vol. 98, no. 5, pp. 649 – 665, May 2010.
- [8] I. Corbella, F. Torres, N. Duffo, V. González-Gambau, M. Pablos, I. Duran, and M. Martín-Neira, “First results on MIRAS calibration and overall SMOS performance,” in *11th Specialist Meeting on Microwave Radiometry and Remote Sensing of the Environment (MicroRad)*, March 2010, pp. 1 –4.

- [9] A. Carlström, J. Christensen, P. Ingvarson, J. Embretsén, A. Emrich, and P. de Maagt, “Geostationary Atmospheric Sounder (GAS) demonstrator development,” in *3rd European Conference on Antennas and Propagation (EuCAP)*, March 2009, pp. 2036–2040.
- [10] J. Christensen, A. Carlström, H. Ekström, P. de Maagt, A. Colliander, A. Emrich, and J. Embretsén, “GAS: the Geostationary Atmospheric Sounder,” in *IEEE International Geoscience and Remote Sensing Symposium (IGARSS)*, July 2007, pp. 223–226.
- [11] B. Lambrigtsen, A. Tanner, T. Gaier, P. Kangaslahti, and S. Brown, “Developing a GeoSTAR science mission,” in *IEEE International Geoscience and Remote Sensing Symposium (IGARSS)*, July 2007, pp. 5232–5236.
- [12] A.B. Tanner, S.T. Brown, S.J. Dinardo, T.M. Gaier, P.P. Kangaslahti, B.H. Lambrigtsen, W.J. Wilson, J.R. Piepmeier, C.S. Ruf, S.M. Gross, B.H. Lim, S. Musko, and S. Rogacki, “Initial results of the GeoSTAR prototype (Geosynchronous Synthetic Thinned Array Radiometer),” in *IEEE Aerospace Conference*, 2006.
- [13] D.W. Hawkins, *Digital lag (XF) correlator theory*, January 2004.
- [14] “Ultrafast 3.3 V/5 V Single-Supply SiGe Comparators,” Tech. Rep., Analog Devices, One Technology Way, P.O. Box 9106, Norwood, MA 02062-9106, U.S.A., May 2009.

Part II

PAPERS

PAPER I

Erik Ryman, Anders Emrich, Johan Embretsen, Johan Riesbeck, Stefan Back

Andersson, Per Larsson-Edefors and Lars Svensson

Digital Cross-Correlators: Two Approaches

GigaHertz Symposium

Lund, Sweden

March 9-10, 2010

PAPER II

Erik Ryman, Per Larsson-Edefors, Lars Svensson, Anders Emrich and Stefan
Back Andersson

A Single-chip 64 Input Low Power High Speed Cross-Correlator for Space Application

Microwave Technologies and Techniques Workshop

Noordwijk, The Netherlands

May 10-12, 2010

PAPER III

Erik Ryman, Anders Emrich, Stefan Back Andersson, Johan Riesbeck, Lars
Svensson and Per Larsson-Edefors
**3.6-GHz 0.2-mW/ch/GHz 65-nm Cross-Correlator for
Synthetic Aperture Radiometry**
IEEE Custom Integrated Circuits Conference
San Jose, California, USA
September 18-21, 2011

XS